Peer-reviewed version available at *Pharmaceutics* **2020**, *12*, 872; doi:10.3390/pharmaceutics12090872

Article

Low vacuum filtration method as an alternative extracellular vesicle concentration method: comparison with ultracentrifugation and differential centrifugation

Anna Drożdż [1,2], Agnieszka Kamińska [1], Magdalena Surman [3], Agnieszka Gonet-Surówka [4], Robert Jach [5], Hubert Huras [6], Małgorzata Przybyło [3], Ewa Łucja Stępień [1*]

[1] Department of Medical Physics, Marian Smoluchowski Institute of Physics, Faculty of Physics, Astronomy and Applied Computer Science, Jagiellonian University, Krakow, Poland; anna.drozdz@uj.edu.pl (AD); agnieszka1.kaminska@uj.edu.pl (A.K); e.stepien@uj.edu.pl (E.Ł.S)

[2] Malopolska Centre of Biotechnology, Jagiellonian University, Krakow, Poland

[3] Department of Glycoconjugate Biochemistry, Institute of Zoology and Biomedical Research, Jagiellonian University, Krakow, Poland; magdalena.surman@doctoral.uj.edu.pl (M.S); malgorzata.przybylo@uj.edu.pl (M.P.)

[4] Department of General Chemistry, Faculty of Chemistry, Jagiellonian University, Krakow, Poland; agnieszka.gonet-surowka@uj.edu.pl

[5] Department of Gynecological Endocrinology, Faculty of Medicine, Jagiellonian University Medical College, Krakow, Poland; robert.jach@uj.edu.pl

[6] Department of Obstetrics and Perinatology, Faculty of Medicine, Jagiellonian University Medical College, Krakow, Poland; hubert.huras@uj.edu.pl

* Correspondence: e.stepien@uj.edu.pl

Abstract: Recent years brought great focus in the field of development of extracellular vesicles (EVs) based drug-delivery systems. Considering possible applications of EVs as a drug carriers the isolation process is a crucial step. To solve problems related with EV isolation, we created and validated a new EVs isolation method – Low Vacuum Filtration (LVF) and compared it with two commonly applied procedures - differential centrifugation (DC) and ultracentrifugation (UC). EVs isolated from endothelial cells culture media have been characterized by a) transmission electron microscopy (TEM) b) nanoparticle tracking analysis (NTA), c) western blot and d) Fourier-Transform Infrared Spectroscopy (FTIR). Additionally, the membrane surface have been imaged with Environmental Scanning Electron Microscopy (ESEM). We showed that LVF is reproducible and efficient method for EVs isolation form conditioned media. Additionally, we observed correlation between ATR-FTIR spectra quality and the EVs and proteins concentration. ESEM imaging confirmed that actual pore diameter are close to the values calculated theoretically. LVF method is an easy, fast and inexpensive EVs isolation method which allows for isolation of both ectosomes and exosomes from high volume sources with good repeatability. We think that it could be an efficient alternative for commonly applied methods.

Keywords: dialysis membrane, ectosomes, exosomes, FTIR, infrared spectroscopy, purification

1. Introduction

Extracellular vesicles (EVs) are defined as bilayer cell membrane fragments, released into the extracellular space [1]. Amount and composition of EVs can vary, depending on the cells they originate from and the physiological or pathological conditions [2, 3]. In experimental conditions, EVs are released to cell culture media, producing conditioned medium [4, 5, 6, 7]. Classification of EVs is based mostly on the way they are formed and released. Large variation in size, composition and function has been recognized among three types of EVs (Table.1).

Table. 1. Characterization of EVs population according to the: diameter, biogenesis, physiological role, cargo and typical markers.

	Exosomes	Ectosomes	Apoptotic bodies
Diameter	30-100 nm	100-1000 nm	1000-5000 nm
Release mechanism	Inside the cell in multivesicullar bodies	On the cell surface, blebbing of the cell membrane	Cell fragments, generated during cell apoptosis
Role	Cell to cell communication	Cell to cell communication	Phagocytosis facilitation
Cargo	DNA, RNA, proteins [8]	DNA, RNA, proteins [8]	Cell organelles, nuclear fraction [9]
Markers	Tetraspanins: CD9, CD63, CD81, Hsp70, Hsp90, Alix, Tsg 101, flotilin [10, 11, 12]	Integrins, selectins, ARF 6 [13, 14]	Thrombospondin and C3b [15]

EVs are widely studied because of their involvement in cell-to-cell communication [16], tumor progression [17], possible application as biomarkers [18] or drug delivery systems (DDS) [19]. While studying functional differences between the different types of EVs, it is crucial to use an adequate isolation method, which allows to obtain homogenous EV population. Unfortunately, it is challenging and the contamination of different EV types is very often observed [20].

An additional difficulty is the isolation of EVs from large volume sources, or when high amount of EVs is required for the downstream analysis. In 2016, a worldwide study on applied EVs isolation methods has been performed among the members of International Society of Extracellular Vesicles (ISEV) [21]. The study showed that 81 % of respondents isolate EVs from conditioned media. Additionally, 71% of respondents isolate EVs from sources which starting volumes exceeding 5 ml (even up to 100 ml). According to this study, the most popular method is ultracentrifugation (81% of respondents) for which the processing of high-volume samples can be difficult, because of the relatively small size of the usually used ultracentrifuge tubes. Moreover, ultracentrifugation is a low yield method and is characterized by high levels of contamination due to the co-precipitation of proteins [22, 23, 24].

Working with high volume sources e.g. conditioned cell culture media, we propose a new method of EVs isolation that allows for EVs concentration in a relatively short time. Low vacuum filtration (LVF) method is a modification of hydrostatic filtration dialysis (HFD method) described by Musante et al. [25] – extended with the application of low vacuum (-0.3 Bar) in order to obtain faster filtration, which can limit the influence of isolation time on the changes in the sample [26]. The filtration system (Figure. 1) consists of the closed cell culture media container (a in Figure. 1) from which, through the coupler (b in Figure. 1), cell culture media flows into a dialysis membrane (c in Figure. 1), where filtration is facilitated by a negative pressure generated by pump (f in Figure. 1) in the vacuum chamber (d in Figure. 1). The dialysis membrane is closed with the clamp (e in Figure. 1) at the end. During the filtration process, EVs accumulate inside the membrane and cell culture media flows thought the micropores which leads to the sample concentration. The final volume of a sample may be reduced down to 1 ml. Using an additional step of membrane washing, the reduction of protein contamination in the sample can be achieved.

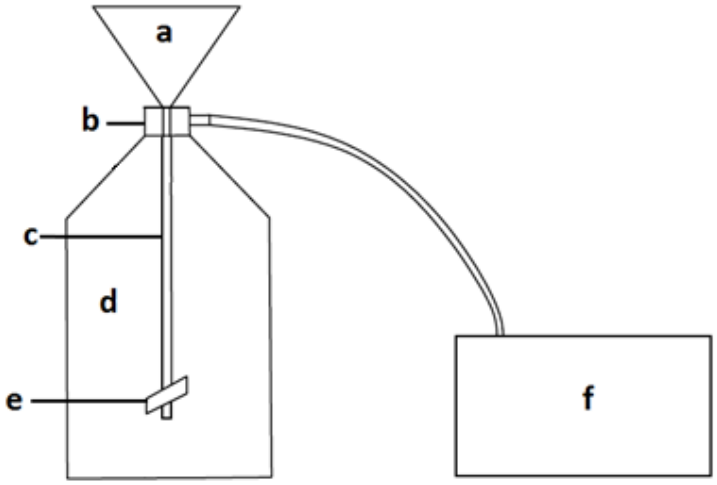

Figure. 1. Low vacuum filtration system: a) closed liquid container, b) the coupler - element connecting the dialysis membrane with liquid container, c) the dialysis membrane, d) the vacuum chamber, e) clamp closing the membrane, f) the pump.

The aim of this study was comparison of effectiveness of three methods of EV isolation: the LVF, differential centrifugation and ultracentrifugation. EVs were isolated from Human Umbilical Endothelial Vein Cells (HUVEC) conditioned media and the obtained EV samples were compared in terms of the following parameters: size distribution, morphology, concentration and homogeneity of the EVs populations. We also applied Fourier Transform Infrared Spectroscopy (FTIR) for EV molecular characterization in order to assess biochemical components as the reproducibility indicators of the method.

2. Materials and Methods

2.1. Cell culture

Umbilical cords were collected during C-section performed between 38 and 42 week of normal pregnancy and stored in HANKS balance salt solution at 4°C until HUVEC isolation. For cell digestion, an umbilical vein was injected with pre-warmed (37°C) 0.25% trypsin (cat. No. 85450C, Sigma Aldrich) with EDTA (380 mg/l) (cat. No. E6758, Sigma Aldrich) mixed with cell culture medium 199 (cat. No. M7653, Sigma Aldrich) (1:1). Umbilical cords were incubated at 37°C in PBS for 30 minutes; afterwards the cells were washed out from the vein, collected in a 50 ml Falcone tube and centrifuged at 250 g for 15 min. The cell pellet was suspended in culture medium and cells were seeded into culture flasks.

HUVECs were cultured in a 75 cm2 flask with the 1:1 mixture of 199 medium and SFM (Human Endothelium Serum Free Medium, cat. No. 11111044, GIBCO), supplemented with 10% of FBS (Fetal Bovine Serum, cat. No. S181B-500, Biowest), penicillin/streptomycin (cat. No. P0781 BioReagent) at concentration of 10 000 units/l (penicillin) and 1 mg/l (streptomycin) and 2 mM L-glutamine (cat. No. 17-605E, BioWhitaker, Lonza).

Before the sample collection HUVECs were serum starved for 24 h to obtain synchronization and avoid contamination by serum EVs [27, 28]. Conditioned media were pulled from twelve bottles and divided into three equal portions for each method of isolation to obtain the same starting material composition in volume of 40 ml.

2.2. Extracellular vesicle isolation

Every sample, before the procedure, underwent three preparatory centrifugations (Figure. 2). In order to remove intact cells, cell debris and apoptotic bodies, samples were centrifuged subsequently at 400 g (10 min), 3,100 g (25 min) and 7,000 g (20 min) at 4°C.

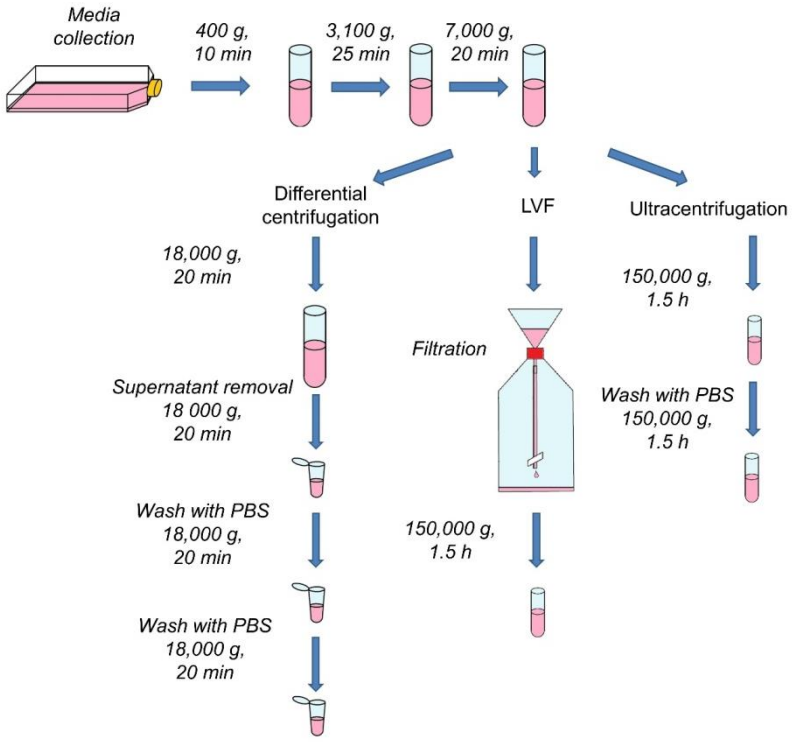

Figure. 2. Scheme of the experiment design. After conditioned media collection, samples underwent introductory centrifugations to remove cells, cell fragments and apoptotic bodies. After the preliminary steps, EVs were isolated according to the procedure for each method.

2.2.1. Ultracentrifugation (UC)

After the initial centrifugation steps, samples were transferred to 1.5 ml top-opened centrifuge tubes and span for 1.5 hours at 150,000 g at 4°C (Sorvall MX 150+ Micro-Ultracentrifuge, Thermo Scientific). EV pellets were suspended in 50 µl of PBS, collected into one tube and span once again under the same conditions. Samples were prepared in triplicates and pellets were stored at −80°C for a downstream analysis.

2.2.2. Differential centrifugation (DC)

Differential centrifugation was performed according to the previously described protocol [29]. After the three introductory centrifugations samples were transferred to 50 ml polycarbonate centrifuge tubes and centrifuged for 20 min at 18,000 g at 4°C (Sorvall LYNX 6000 Superspeed Centrifuge, Thermo Scientific). Part of the supernatant was discarded and the lower part of medium (1.5 ml) was centrifuged in eppendorf tubes under the same conditions (5804 R centrifuge, Eppendorf). The pellets were resuspended in 1.5 ml of PBS, and centrifuged again two times under the same conditions (Figure. 2). Samples were prepared in triplicates and pellets were stored at −80°C for the downstream analysis.

2.2.3. Low vacuum filtration (LVF)

LVF was performed on the dialysis membrane (cat. No. 131486, Spectra/Por Biotech) with MCWO = 1000 kDa. The whole system was assembled as presented in Figure. 1. After the

preliminary centrifugations, 40 ml of sample was placed in the liquid container (a in Figure. 1), filtered under low vacuum (-0,3 Bar) and subsequently washed with 15 ml of water. After the filtration, samples, which were prepared in triplicates, were stored at −80°C for the downstream analysis. For the purpose of TEM imaging, samples after the filtration were ultracentrifuged under the conditions described in 2.2.1. section.

2.3. Environmental Scanning Electron Microscopy

To evaluate the pores diameter of the dialysis membrane, we applied Environmental Scanning Electron Microscopy (ESEM). A fragment of the dialysis membrane (1 x 1 cm) was placed on the SEM sample holder and the subsequent ESEM measurements were performed using the SEM Quanta 3D FEG microscope (FEI Company, USA) in use by the Department of Solid State Physics (Institute of Physics Jagiellonian University, Kraków, Poland). The ESEM images were collected by LVED (Low Vacuum Secondary Electron Detector) detector using an electron beam of 20 keV energy. During the measurement specimen was kept at 130 Pa of water vapor at room temperature.

2.4. Transmission Electron Microscopy

Samples for the TEM imaging were prepared as previously described [18]. Pellets of isolated EVs were fixed with 2.5% glutaraldehyde (cat. No. G5882, Sigma-Aldrich) in 0.1 M cacodylic buffer (cat. No. C4945, Sigma Aldrich) and then postfixed in 1% osmium tetroxide solution for 1 hour. In the next step, samples were dehydrated in ethanol and embedded in PolyBed 812 (cat. No. 08792-1, Polysciences) at 68°C. Ultrathin sections were placed on the 300 mesh grids, covered with formvar film, and contrasted using uranyl acetate and lead citrate. Observations were performed on the JEOL JEM2100HT (Jeol Ltd) electron microscope with the accelerating voltage equal to 80 kV.

Images were analyzed using Photoshop and CTAnalyzer software. Background was removed from the binarized images and EVs as single objects were counted automatically. Four different parameters were considered: diameter, area, solidity and eccentricity. Solidity was calculated according to the equation:

$$solidity = \frac{area}{area\ created\ by\ convex\ hull},$$

This is a parameter describing the extent to which a shape is convex or concave. This parameter is equal to 1 for the shape with no irregularities and convex, and 0 for the shape with many thin insets and concavity [30]. Eccentricity, calculated according to the equation:

$$eccentricity = \frac{minor\ axis\ lenght}{major\ axis\ lenght},$$

compares length of minor axis and major axis which gives information about the changes in the elongation of an object.

2.5. Nanoparticle Tracking Analysis

NTA measurements were performed by means of the NanoSight LM 10 (Malvern Panalytical), coupled with a 405 nm laser. For the NTA analysis, 100 µl of each sample was diluted to the volume of 500 µl with filtered PBS. For each method, three samples were prepared and measured in five independent records for 30 s. The measurements were analyzed using the NTA 3.1. software, calculated and normalized to the starting sample volumes. The final results were analyzed by means the OriginPro 2018 Software.

2.6. Fourier-transform infrared spectroscopy - FTIR

For the FTIR spectroscopy measurements, 5 µl of each sample in PBS was mounted and dried on the diamond crystal of the Nicolete 6700 FT-IR spectrometer (Thermo Scientific) to obtain a thin dry film. Measurements were performed immediately at room temperature and 256 scans were

collected at a nominal resolution of 4 cm− 1. The analysis of obtained spectra was performed using the OriginPro 2018 Software.

2.7. Electrophoresis and western blot

EV protein extracts (15 μg per sample) were diluted 1:1 in the Laemmli Sample buffer (62.5 mM Tris-HCl, pH 6.8, 1 mM EDTA, 10% glicerol, 2% SDS, 0.025% bromophenol blue with 5% β-mercaptoethanol), separated by electrophoresis using the 4-15% gradient Mini-PROTEAN TGX Stain-Free Protein Gels (cat. Number 4568085, BioRad Laboratories Inc.) and transferred to PVDF membranes using the Mini-Protean 3 system (Bio-Rad Laboratories Inc.).

Western blot analysis was performed using Lumi-LightPLUS Western Blotting Kit (Mouse/Rabbit) (cat. No. 12015218001, Roche). The blots were blocked overnight in 1% BSA in TBS/Tween buffer (0.05 M Tris-HCl, 0.15 M NaCl, 0.1% Tween 20, pH 7.5, Lumi-LightPLUS Western Blotting Kit (Mouse/Rabbit) and incubated for 1 h with primary antibodies against VCAM (dilution 1:500, cat. No. sc-13160, Santa Cruz Biotechnology, Inc), Hsp70 (dilution 1:500, cat. No. sc-24, Santa Cruz Biotechnology, Inc.) and ARF- 6 (dilution 1:200, cat. No. sc-7971, Santa Cruz Biotechnology, Inc.). After incubation with the primary antibodies, membranes were washed three times with Tween/TBS buffer and incubated for 1 h with an appropriate HRP-conjugated secondary antibody (Lumi-LightPLUS Western Mouse/Rabbit Blotting Kit) diluted 1:250 in 1% BSA in TBS/Tween buffer. Afterwards, incubation membranes were washed three times in the TBS/Tween Buffer and three times in the TBS buffer (0.05 M Tris-HCl, 0.15 M NaCl, pH 7.5. Immunopossitive bands were visualized using Lumi-light Reagent (Roche) and ChemiDoc™ XRS+ System (Bio-Rad Laboratories Inc.). The relative levels of protein expression were determined using Lab Image software. Individual protein levels were normalized to the total intensity of the bands on a given line, detected in the gel after electrophoresis.

2.8. Ethical statement

Collection of umbilical cords for this study was approved by The Bioethical Committee of Jagiellonian University in Kraków on 26 April 2016 . The permission number 122.6120.78.2016 was valid until 30 April 2016.

3. Results

3.1. Evaluation of dialysis membrane pores diameter with ESEM

ESEM was used to visualize pores in the dialysis membrane. Figure. 3 shows an exemplary image obtained in ESEM. ESEM measurements reveal irregular structure of the membrane with pores with different diameters (ranging from 20.59 nm to 51.05 nm). The average pore size calculated from the 50 randomly selected pores was 28.39 ± 9.63 nm

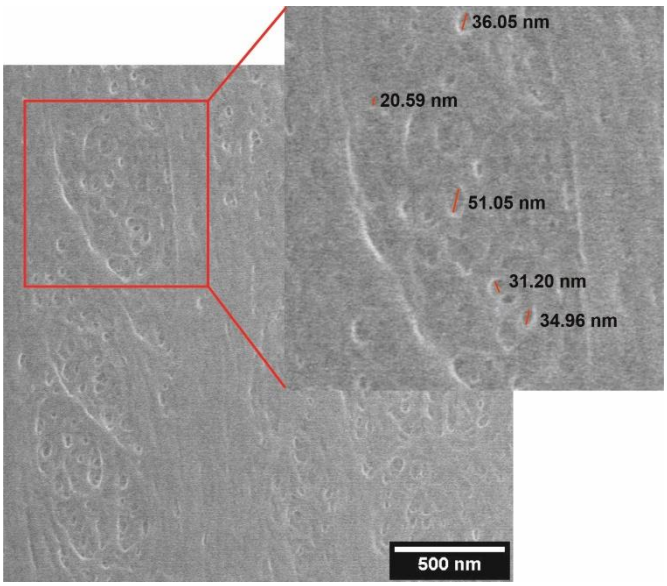

Figure. 3. An exemplary ESEM micrograph of the dialysis membrane surface, with the measurement of the sizes of several pores.

3.2. EVs visualization with TEM

TEM was used to confirm the presence of EVs in the analyzed samples. Figure. 4 shows the representative images of EVs isolated with differential centrifugation (a in Figure. 4), LVF (b in Figure. 4) and ultracentrifugation (c in Figure. 4). Additionally, in order to investigate the influence of applied methods on the EVs morphology we compared their area, eccentricity and solidity.

The highest amounts of particles detected in the TEM samples were observed for EVs isolated by differential centrifugation (52 particles/image) and LVF method (18 particles/image); the lowest amounts was for samples isolated by ultracentrifugation (5 particles/image). Additionally, the electron density of EVs was highest for the LVF method and lowest for the ultracentrifugation. The average diameter of EVs and size distribution varied between samples (Figure. 4). The largest EVs with the average diameter of 227 ± 175 nm and median diameter of 175 nm were observed in the samples isolated by differential centrifugation. In samples obtained by LVF, EVs had the average diameter of 114 ± 69 nm and the median diameter of 100 nm. In ultracentrifugation samples, the smallest EVs were observed with the average diameter of 78 ± 44 nm and median diameter of 72 nm. The area of EVs corresponded to the mean diameter, as well as shape parameters, which were very similar among analyzed groups (Tables in Figure. 4). For each isolation method we observed elongation of the samples – eccentricity parameter varies between 0.57 ± 0.15 for the centrifugation and 0.60 ± 0.15 for LVF. We have not observed differences in the solidity of particles. In the differential centrifugation and LVF isolation, EVs had the same solidity of 0.92 ± 0.07 and 0.92 ± 0.07, respectively. EVs isolated by the ultracentrifugation had lower solidity of 0.91 ± 0.02.

Preprints (www.preprints.org) | NOT PEER-REVIEWED | Posted: 27 July 2020 doi:10.20944/preprints202007.0655.v1

Peer-reviewed version available at Pharmaceutics 2020, 12, 872; doi:10.3390/pharmaceutics12090872

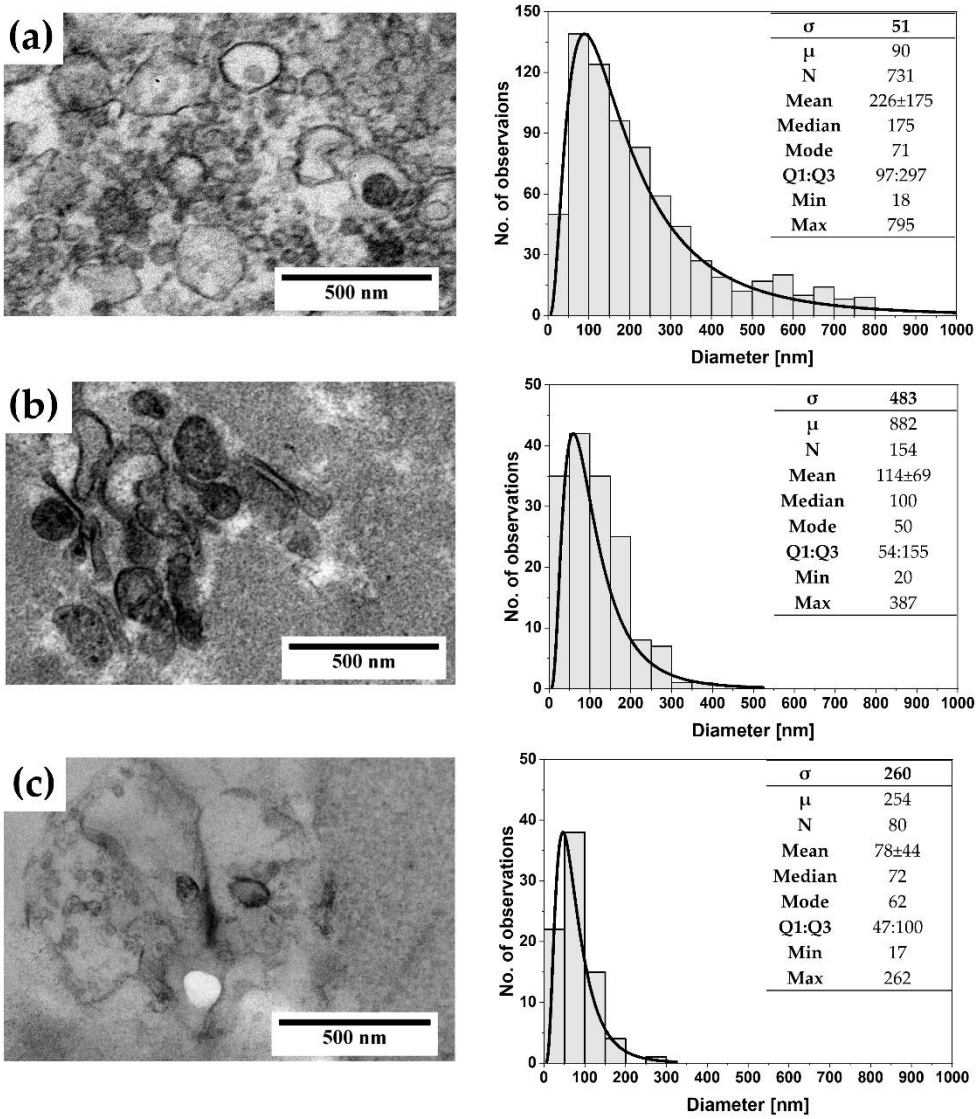

	Area [nm²]	Eccentricity [-]	Solidity [-]
Differential centrifugation	44193 ± 72727	0.58 ± 0.16	0.92 ± 0.07
LVF	12231 ± 12018	0.6 ± 0.15	0.92 ± 0.03
Ultracentrifugation	4647 ± 3918	0.57 ± 0.15	0.91 ± 0.02

Figure. 4. Representative TEM images and size distributions, with the log-normal fit parameters, for the EVs isolated by: differential centrifugation (A), LVF (B), ultracentrifugation (C); below: a table summarizing average area, eccentricity and solidity of the EVs obtained by three different isolation methods.

3.3. NTA measurements of EVs concentration and size

EVs concentrations were measured for the starting samples and for the samples after isolation, using NTA analysis. The average concentrations of EVs in the samples after ultracentrifugation were 1.71*1010 ± 1.23*108 particles/ml. The average size of detected EVs was 224 ± 112 nm and EVs with diameter lower than 100 nm were not detected. We observed the 35-times increase in the EV concentration in comparison to the starting sample.

For samples isolated by the LVF method, the average concentrations of EVs were 7.96*109 ± 5.82*107 particles/ml. The average size was equal to 260 ± 132 nm and the particles with diameter

lower than 100 nm were also not detected. We observed a 22-times increase in particles concentration in comparison to starting sample.

The lowest concentrations were measured for the samples obtained after differential centrifugation - 4.74*109 ± 3.91*107 particles/ml. Average size was equal to 255 ± 142 nm, in contrast to the other methods, EVs with the diameter lower than 100 nm were detected. We observed a 13-times increase in the EV concentration in comparison to the starting sample. High variations in size and concentration were observed (Figure. 5).

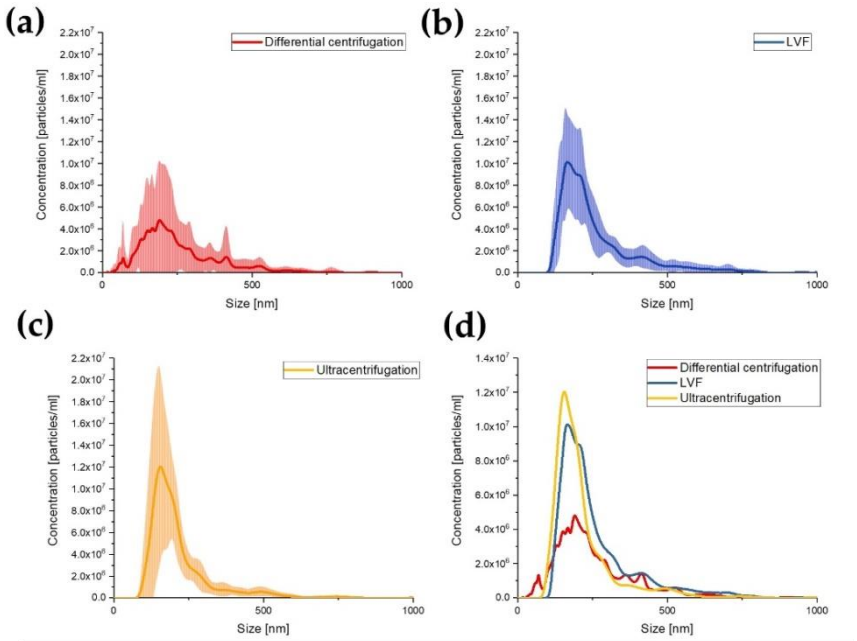

Method	Concentration [particles/ml]	Sample condensation	Mean size [nm]	Size mode [nm]
Differential centrifugation	$4.74*10^{9}$±$3.91*10^{7}$	13x	255±142	167
LVF	$7.96*10^{9}$±$5.82*10^{7}$	22x	260±132	184
Ultracentrifugation	$1.71*10^{10}$±$1.23*10^{8}$	35x	224 ±112	170

Figure. 5. Results of the NTA analysis. A – Differential centrifugation, B – LVF, C – ultracentrifugation, D – comparison among tested isolation methods. Results are presented as an average concentration (line) of the three samples. Each sample was recorded for 30 s and the measurement was repeated 5 times. SD of the three independent measurements is presented as the brightened lines around the mean concentration line. The table presents the average concentrations of EVs in the samples after isolation, the parameter of sample condensation, defined as a relative increase in the number of the EVs in the sample after isolation, compared to their concentration in the starting samples, an average diameter and the size mode.

3.4. Infrared spectra of EVs

Infrared (IR) spectroscopy provides general information about sample chemical composition giving additional details regarding the quality of isolated EVs, especially in context of the protein and lipids content. Two amide peaks (amide I and amide II) are the main components of the EV infrared spectra
(Figure. 6). In the tested samples, these two peaks originating from peptides: the amide I band, at around 1652 cm-1 [31] and the amide II band, at around 1542 cm-1 [31] were distinguished. Additionally, the peak at around 3286 cm-1 belonging to amide A [31] was observed. The highest intensity for those peaks, associated with proteins and peptides, was detected for the EVs isolated by LVF and ultracentrifugation. In differential centrifugation samples, those peaks were barely distinguished and with low intensity. In the LVF samples, additional peaks were observed at 1309 cm-1 and 1240 cm-1, which are attributed to amide III (C-N stretching mode of proteins).

Lipids bands are represented as four peaks originating from the stretching vibrations of lipid acyl chain groups. The peaks at 3076 cm-1 and 2959 cm-1 are generated by the CH3 asymmetric stretching, while the peaks around 2930 cm-1 and 2869 cm-1 are generated by the CH2 asymmetric and symmetric stretching vibrations. Additional lipids peaks can be distinguished around 1450 cm-1 and 1397 cm-1, originating from the CH2 [32] and the CH3 [32] bending vibrations, respectively, in the lipid acyl chains. Similarly as in the case of the protein bans, lipids bands were detected in the LVF and ultracentrifugation samples and were barely distinguishable in the samples of the EVs isolated by differential centrifugation.

Table. 2. FTIR peaks assignment.

Wavenumber [cm^{-1}]	**Definition of the spectra assignment**
3286	Overlapped –OH stretching vibrations and N-H stretching vibrations from peptide groups of proteins (amide A) [31]
3076 2959	CH_3 asymmetric stretching vibrations from lipids with low contribution from proteins, carbohydrates, nucleic acids [33]
2930 2869	CH_2 asymmetric and symmetric stretching vibrations from lipids with low contribution from proteins, carbohydrates, nucleic acids [34]
1652	C=O stretching vibrations from peptide backbone (amide I) [31]
1542	N-H bending vibrations from the peptide groups (amide II) [31]
1450	CH_2 bending (scissoring) vibrations from lipid acyl [32]
1397	CH_3 bending vibrations from lipids and proteins [32]
1309 1240	C-N stretching mode of proteins, indicating mainly α-helix conformation (amide III) [35]

In order to perform further peak analysis for amide (1450 – 1750 cm-1) and lipid (2800 – 3000 cm-1) bands, automatic baseline subtraction and the Gauss function fittings were performed to all peaks in the analyzed ranges. Based on the value of areas under the curves the amide I/lipids ratio was calculated and the highest ratio was obtained for the LVF and ultracentrifugation samples: 10.22 and 6.31, respectively. IR spectra for EVs isolated with differential centrifugation were characterized with the lowest ratio (4.15) and the total area under analyzed peaks was much lower than for other samples.

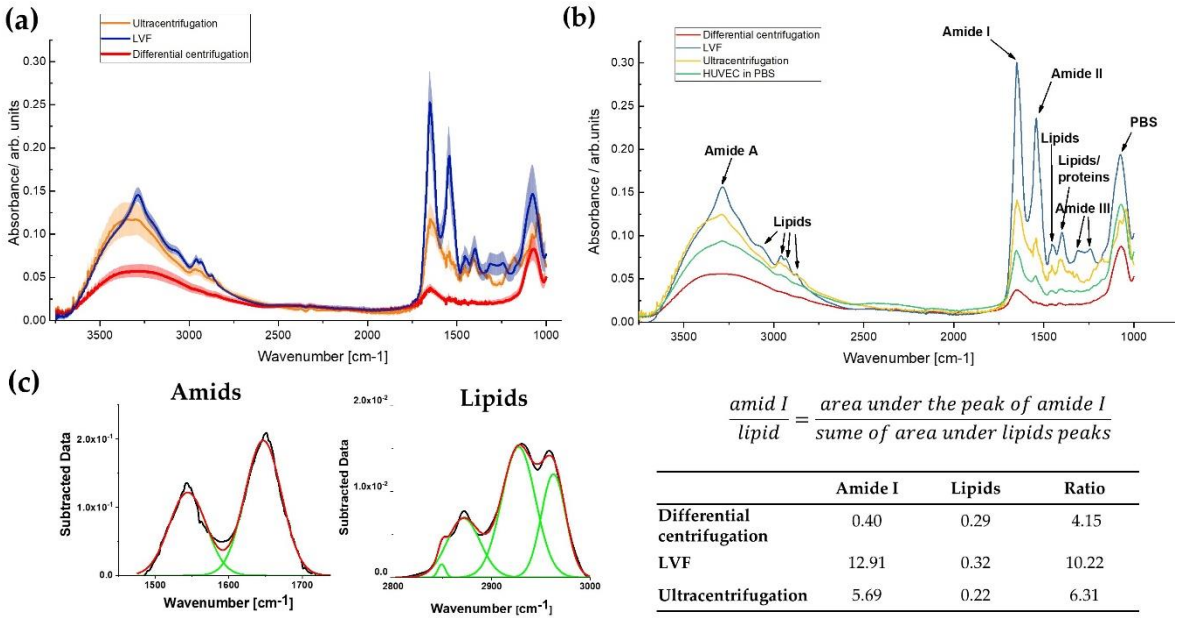

$$\frac{amid\ I}{lipid} = \frac{area\ under\ the\ peak\ of\ amide\ I}{sume\ of\ area\ under\ lipids\ peaks}$$

	Amide I	Lipids	Ratio
Differential centrifugation	0.40	0.29	4.15
LVF	12.91	0.32	10.22
Ultracentrifugation	5.69	0.22	6.31

Figure. 6. Results of the FTIR analysis. (A) Average infrared spectra for EVs isolated with the tested methods (line) with SD of three independent measurements (brightened lines). (B) Comparison of the EVs spectra with, the spectra of HUVEC cells with the assignment of the main peaks. (C) Example of the Gauss function fitting for amide I/lipids ratio calculation with results (table).

3.5. EV protein markers

In order to investigate the type of EVs present in the isolated samples Western blot analysis was performed. The total protein amount in the EV samples was measured by the BCA method and the highest protein concentration was stated in the LVF samples (3.73 ± 0.63 mg/ml). In the ultracentrifugation and differential centrifugation samples, protein amounts were similar: 2.41 ± 1.70 mg/ml and 2.40 ± 0.23 mg/ml, respectively (Figure. 7). To confirm the endothelial origin of the isolated EVs, vascular cell adhesion molecule 1 (VCAM-1) was used as an endothelial marker. High intensity bands for VCAM-1 were observed in the differential centrifugation and LVF samples: 1.50 ± 0.16 AU and 1.38 ± 0.24 AU, respectively. The intensity of these bands was significantly higher than in the ultracentrifugation samples (0.89 ± 0.11 AU).

As an ectosomal marker Arf-6 was used and Arf-6-positive bands were detected with low intensity for all tested samples (differential centrifugation – 0.7 ± 0.02 AU, LVF – 0.5 ± 0.02 AU, ultracentrifugation – 0.7 ± 0.04 AU). As an exosome marker Hsp70 was used and bands of high intensity were detected in the LVF samples (0.48 ± 0.14 AU), compared to the ultracentrifugation and differential centrifugation samples: 0.23 ± 0.12 AU vs. 0.04 ± 0.01 AU, $p < 0.05$.

Preprints (www.preprints.org) | NOT PEER-REVIEWED | Posted: 27 July 2020 doi:10.20944/preprints202007.0655.v1

Peer-reviewed version available at Pharmaceutics 2020, 12, 872; doi:10.3390/pharmaceutics12090872

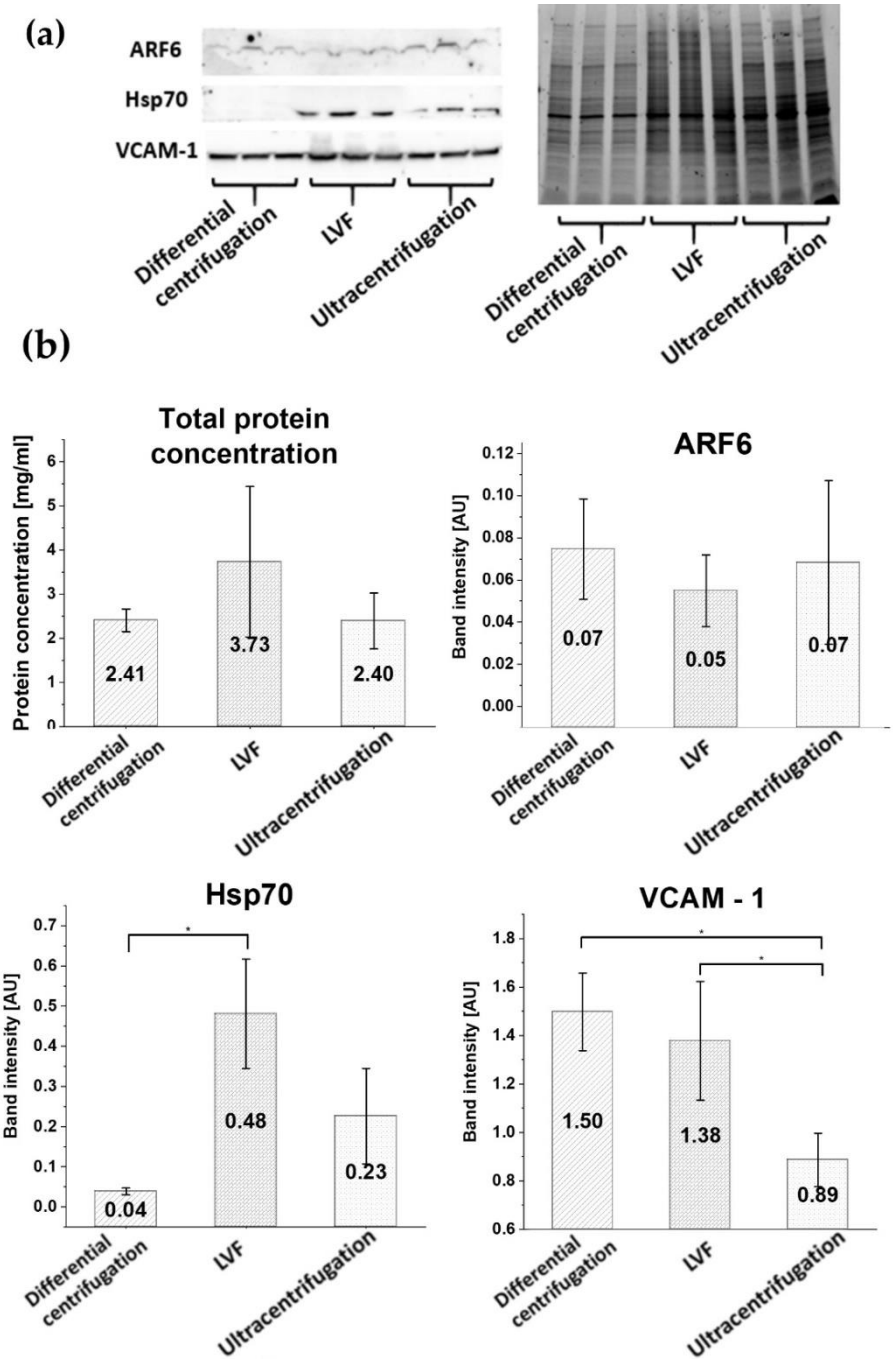

Figure. 7. Results of the western blot analysis. (A) Images of the membrane after blotting and a gel after electrophoresis with clearly visible differences in bands intensities in the EV samples isolated by different methods. (B) Analysis of band intensity. Data are presented as mean values (column) with SD (whiskers). The analysis was performed using Kruskal-Wallis test. Differences between subgroups were tested with Dunn's post hoc test and statistically significant differences are marked with an asterisk ($p < 0.05$).

4. Discussion

The interest in the extracellular vesicles has grown over the last years [36], mostly because of their involvement in cell-to-cell communication [37], cancer progression [38], immunosuppression [39] as well as their great potential as DDS [40]. Besides recent intense development in EV isolation micromethods, there is an unmet need to develop more efficient and repeatable isolation and concentration methods from high volume sources, suitable not only for proteomic analysis but also

for the drug delivery purposes [41]. In this study, we developed and validated a system which is dedicated for concentration of EVs from high volume sources – conditioned media: Low Vacuum Filtration (LVF).

As we showed in this study, EVs can be concentrated from high volume culture supernatants on the dialysis membranes (MWCO = 1000 kDa), by means of the LVF method. We also compared EVs isolated using LVF, with two most commonly used alternative methods: ultracentrifugation and differential centrifugation [22] and showed that both protein and lipid contents were higher in the LVF samples in comparison to other isolation methods. FTIR spectroscopy was used for assessing quality and repeatability of EVs isolation and molecular content analysis.

It has been reported that ultrafiltration is a good alternative to the ultracentrifugation method [22, 23, 24]. However, isolation of EVs through filtration could be challenging, mainly due to need of rinsing EVs from the membrane with additional chemical compounds [43], membrane pores plugging resulting in the low yield of isolation [44] and possible changes in EVs' morphology due to the application of high pressure [45] as well as time consuming procedures [25]. LVF method can solve these problems, because of important amenities. There is no need to wash EVs from the membrane using chemical compounds, as only water is used to rinse additional proteins from the sample. Membrane plugging, prevalent in other methods, was also not observed in our method. The yield of isolation of the LVF method is comparable with ultracentrifugation and significantly better than the yield of isolation of the differential centrifugation method (shown in Figure. 5). As compared to the initial sample, EVs concentration was 35 times higher in the case of ultracentrifugation procedure, 22 times higher concentration in the case of the LVF method and 12 times higher than in the case of differential centrifugation. Moreover, we assessed the impact of applied pressure on the EV shape by means of TEM imaging and we did not observe any EV shape deformations in the LVF samples (defined through the shape parameters: eccentricity and solidity – shown in Figure. 4). Another advantage of the LVF method is the isolation time. In our method, pressure is used to facilitate filtration and can speed up filtration process up to 4 times (for 100 ml from 8 hours for the standard methods to 2 hours with an addition of an additional pressure). This speed of isolation is unavailable for high volume sources without dedicated centrifuges.

Diameter of membrane pores, measured by means of ESEM, varied between 20 and 50 nm. TEM images of LVF samples confirmed the presence of EV with the minimal diameter of 20 nm (TEM, Figure. 4), while the NTA analysis showed the presence of EV with minimal diameter of 66 nm (raw data). Therefore, we can assume that even the smallest EVs can be retained in the filtered media.

In order to confirm that both ectosomes and exosomes were present in the isolated EV samples, not only by means of the size distribution methods (described above), we applied western blot to detect specific exosome and ectosome markers: Hsp70 and AFR-6, respectively (Figure. 7). We showed that LVF samples had the highest intensity of Hsp70 band, while the ARF-6 bands had similar intensity in the samples isolated by all tested methods. Therefore, we conclude that the samples isolated by LVF contained the highest concentrations of exosomes while the ectosomes concentration was similar in all samples regardless of the isolation method used. It has been postulated that additional centrifugation or filtration steps should be used in order to avoid ectosomal contamination in the ultracentrifugation isolation method [46]. In this study, we observed that bands attributed to the exosome marker in the differential centrifugation samples were more than ten times less intensive than in the case of samples isolated by LVF. Based on our findings, we also recommend to use additional centrifugation at 18,000 g in order to remove ectosomes an additional preliminary centrifugation if the goal is to obtain clear exosomal samples in the next isolation steps in ultracentrifugation, as well as before the concentration by LVF [**错误!未定义书签。**, **错误!未定义书签。**].

We used FTIR in our study as a new approach. Previously it has been shown that FTIR is useful as a screening method for resolving EV protein composition and structure (β-sheet) [32]. In the isolated EV samples, we analyzed three strongest peptide peaks: amide I (1652 cm-1), amide II (1542 cm-1) and amide A (around 3286 cm-1). The highest intensity of these peaks was measured for EVs

isolated by LVF and ultracentrifugation methods. Protein bands were barely distinguishable in the spectra of samples obtained after differential centrifugation. Similarly, to the protein bands, typical lipid bands (3076 cm-1, 2959 cm-1, 2930 cm-1, 2869 cm-1, 1450 cm-1) were clearly visible for the samples isolated with LVF and ultracentrifugation methods. Additionally, in the LVF spectra, additional peaks appear at 1309 cm-1 and 1240 cm-1, which can be attributed to the amide III (C-N stretching mode of proteins). Presence of the amide III peak can indicate the presence of α-helix structures in the sample.

Moreover, we applied the FTIR analysis not only to assess the sample quality but also as a protein concentration indicator (the amide to lipids ratio). Protein concentration correlates with amide I to lipids ratio for LVF and ultracentrifugation samples (compare Figure. 6 and Figure. 7). On the other hand, samples isolated by differential centrifugation and ultracentrifugation had similar protein concentration. Nevertheless, amide to lipids ratio was significantly different. This is probably an result of low quality of samples and low resolution of FTIR spectra, where the peaks were barely distinguishable, nevertheless calculations of area under the curve and the ratio between these two values were still possible.

The FTIR spectra confirm that the LVF method is reproducible, if other possible errors causing factors (temperature, time of processing, pre-analytical errors and human factor) will be controlled.

5. Conclusions

The LVF method can be recommended as a workflow for EVs isolation from conditioned media in high volume samples. This method is easy, fast and low-cost allowing for the isolation of both ectosomes and exosomes from high volume sources and could be an efficient alternative for commonly applied methods. These characteristics, especially high reproducibility, may lead to the future applications of this method as the isolation protocol dedicated for the development of the drug delivery systems based on EVs.

Author Contributions: For research articles with several authors, a short paragraph specifying their individual contributions must be provided. The following statements should be used "Conceptualization, A.D., A.K. and E.Ł.S.; methodology, A.D., A.K., M.S., A.G.-S., M.P. and E.Ł.S ; validation, A.D and E.Ł.S.; formal analysis, A.D. and E.Ł.S.; investigation, A.D. A.K., M.S., A.G.-S. and; resources, R.J. and H.H.; data curation, M.P. and E.Ł.S. ; writing—original draft preparation, A.D.; writing—review and editing, M.P. and E.Ł.S.; visualization, A.D.; supervision, E.Ł.S.; project administration, A.D.; funding acquisition, A.D. and E.Ł.S. All authors have read and agreed to the published version of the manuscript.", please turn to the CRediT taxonomy for the term explanation. Authorship must be limited to those who have contributed substantially to the work reported.

Funding: This study was funded by the Polish National Science Center (grant no. 2017/25/N/ST5/00831).

Acknowledgments: The Environmental Scanning Electron Microscopy measurement was carried out with equipment purchased with financial support from the European Regional Development Fund in the framework of the Polish Innovation Economy Operational Program (Contract no. POIG.02.01.00-12-023/08). Authors want to express their gratitude to Dr Eng. Olga Woźnicka from the Microscopy Laboratory of the Institute of Zoology and Biomedical Research, the Jagiellonian University in Kraków, for specimen preparation and TEM imaging as well as Dr Konrad Szajna from the Department of Solid State Physics of the Institute of Physics, the Jagiellonian University in Kraków, for ESEM imaging.

Conflicts of Interest: The authors declare no conflict of interest.

References

1. Lawson, C.; Vicencio, J.M.; Yellon, D.M.; Davidson, S.M. Microvesicles and exosomes: New players in metabolic and cardiovascular disease. *J. Endocrinol.* **2016**, *228*, R57–R71, doi:10.1530/JOE-15-0201.
2. Tokarz, A.; Szuścik, I.; Kuśnierz-Cabala, B.; Kapusta, M.; Konkolewska, M.; Żurakowski, A.; Georgescu, A.; Stępień, E. Extracellular vesicles participate in the transport of cytokines and angiogenic factors in diabetic patients with ocular complications. *Folia Med. Cracov.* **2015**, *55*, 35–48.
3. van der Pol, E.; Böing, A.N.; Harrison, P.; Sturk, A.; Nieuwland, R. Classification, functions, and clinical relevance of extracellular vesicles. *Pharmacol. Rev.* **2012**, 64, 676–705, doi:10.1124/pr.112.005983.
4. Sekuła, M.; Janawa, G.; Stankiewicz, E.; Stepień, E. Endothelial microparticle formation in moderate concentrations of homocysteine and methionine in vitro. *Cell. Mol. Biol. Lett.* **2011**, 16, 69–78, doi:10.2478/s11658-010-0040-2.
5. Knudtzon, S.; Mortensen, B.T. Growth stimulation of human bone marrow cells in agar culture by vascular cells**. Blood** *1975,* 46, 937–943 .
6. Durak-Kozica, M.; Baster, Z.; Kubat, K.; Stępień, E. 3D visualization of extracellular vesicle uptake by endothelial cells. *Cell. Mol. Biol. Lett.* **2018**, *23*, 1–9, doi:10.1186/s11658-018-0123-z.
7. Surman, M.; Stępień, E.; Przybyło, M. Melanoma-Derived Extracellular Vesicles: Focus on Their Proteome. *Proteomes* **2019**, *7*, 21.
8. Kim, D.K.; Lee, J.; Kim, S.R.; Choi, D.S.; Yoon, Y.J.; Kim, J.H.; Go, G.; Nhung, D.; Hong, K.; Jang, S.C.; et al. EVpedia: A community web portal for extracellular vesicles research. *Bioinformatics* **2015**, *31*, 933–939, doi:10.1093/bioinformatics/btu741.
9. Fadeel, B.; Orrenius, S. Apoptosis: A basic biological phenomenon with wide-ranging implications in human disease. *J. Intern. Med.* **2005**, *258*, 479–517, doi:10.1111/j.1365-2796.2005.01570.x.
10. Van Deun, J.; Mestdagh, P.; Sormunen, R.; Cocquyt, V.; Vermaelen, K.; Vandesompele, J.; Bracke, M.; De Wever, O.; Hendrix, A. The impact of disparate isolation methods for extracellular vesicles on downstream RNA profiling. *J. Extracell. Vesicles* **2014**, *3*, 1–14, doi:10.3402/jev.v3.24858.
11. Wei, X.; Liu, C.; Wang, H.; Wang, L.; Xiao, F.; Guo, Z.; Zhang, H. Surface Phosphatidylserine Is Responsible for the Internalization on Microvesicles Derived from Hypoxia-Induced Human Bone Marrow Mesenchymal Stem Cells into Human Endothelial Cells. *PLoS One* **2016**, *11*, e0147360, doi:10.1371/journal.pone.0147360.
12. Marie, G.; Dunning, C.J.; Gaspar, R.; Grey, C.; Brundin, P.; Sparr, E.; Linse, S. Acceleration of α-synuclein aggregation by exosomes. *J. Biol. Chem.* **2015**, *290*, 2969–2982, doi:10.1074/jbc.M114.585703.
13. Muralidharan-Chari, V.; Clancy, J.; Plou, C.; Romao, M.; Chavrier, P.; Raposo, G.; D'Souza-Schorey, C. ARF6-Regulated Shedding of Tumor Cell-Derived Plasma Membrane Microvesicles. *Curr. Biol.* **2009**, *19*, 1875–1885, doi:10.1016/j.cub.2009.09.059.
14. Gasser, O.; Hess, C.; Miot, S.; Deon, C.; Sanchez, J.C.; Schifferli, J.A. Characterisation and properties of ectosomes released by human polymorphonuclear neutrophils. *Exp. Cell Res.* **2003**, *285*, 243–257, doi:10.1016/S0014-4827(03)00055-7.
15. Akers, J.C.; Gonda, D.; Kim, R.; Carter, B.S.; Chen, C.C. Biogenesis of extracellular vesicles (EV): exosomes, microvesicles, retrovirus-like vesicles, and apoptotic bodies. *J. Neurooncol.* **2013**, *113*, 1–11, doi:10.1007/s11060-013-1084-8.
16. Frühbeis, C.; Fröhlich, D.; Kuo, W.P.; Amphornrat, J.; Thilemann, S.; Saab, A.S.; Kirchhoff, F.; Möbius, W.; Goebbels, S.; Nave, K.A.; et al. Neurotransmitter-Triggered Transfer of Exosomes Mediates Oligodendrocyte-Neuron Communication. *PLoS Biol.* **2013**, *11*, doi:10.1371/journal.pbio.1001604.
17. Pucci, F.; Garris, C.; Lai, C.P.; Newton, A.; Pfirschke, C.; Engblom, C.; Alvarez, D.; Sprachman, M.; Evavold, C.; Magnuson, A.; et al. SCS macrophages suppress melanoma by restricting tumor-derived vesicle-B cell interactions. *Science (80-.).* **2016**, *352*, 242–246, doi:10.1126/science.aaf1328.
18. Kamińska, A.; Platt, M.; Kasprzyk, J.; Kuśnierz-Cabala, B.; Gala-Błądzińska, A.; Woźnicka, O.; Jany, B.R.; Krok, F.; Piekoszewski, W.; Kuźniewski, M.; et al. Urinary Extracellular Vesicles: Potential Biomarkers of Renal Function in Diabetic Patients. *J. Diabetes Res.* **2016**, *2016*, doi:10.1155/2016/5741518.
19. Munagala, R.; Aqil, F.; Jeyabalan, J.; Gupta, R.C. Bovine milk-derived exosomes for drug delivery. *Cancer Lett.* **2016**, *371*, 48–61, doi:10.1016/j.canlet.2015.10.020.
20. Kowal, J.; Arras, G.; Colombo, M.; Jouve, M.; Morath, J.P.; Primdal-Bengtson, B.; Dingli, F.; Loew, D.; Tkach, M.; Théry, C. Proteomic comparison defines novel markers to characterize heterogeneous populations of extracellular vesicle subtypes. *Proc. Natl. Acad. Sci. U. S. A.* **2016**, *113*, E968–E977, doi:10.1073/pnas.1521230113.

21. Gardiner, C.; Vizio, D. Di; Sahoo, S.; Théry, C.; Witwer, K.W.; Wauben, M.; Hill, A.F. Techniques used for the isolation and characterization of extracellular vesicles: Results of a worldwide survey. *J. Extracell. Vesicles* **2016**, *5*, 1–6, doi:10.3402/jev.v5.32945.
22. Momen-Heravi, F.; Balaj, L.; Alian, S.; Mantel, P.Y.; Halleck, A.E.; Trachtenberg, A.J.; Soria, C.E.; Oquin, S.; Bonebreak, C.M.; Saracoglu, E.; et al. Current methods for the isolation of extracellular vesicles. *Biol. Chem.* **2013**, *394*, 1253–1262, doi:10.1515/hsz-2013-0141.
23. Momen-Heravi, F.; Balaj, L.; Alian, S.; Mantel, P.Y.; Halleck, A.E.; Trachtenberg, A.J.; Soria, C.E.; Oquin, S.; Bonebreak, C.M.; Saracoglu, E.; et al. Current methods for the isolation of extracellular vesicles. *Biol. Chem.* **2013**, *394*, 1253–1262, doi:10.1515/hsz-2013-0141.
24. Abramowicz, A.; Widlak, P.; Pietrowska, M. Proteomic analysis of exosomal cargo: the challenge of high purity vesicle isolation. *Mol. Biosyst.* **2016**, *12*, 1407–1419, doi:10.1039/c6mb00082g.
25. Musante, L.; Tataruch, D.; Gu, D.; Benito-Martin, A.; Calzaferri, G.; Aherne, S.; Holthofer, H. A simplified method to recover urinary vesicles for clinical applications, and sample banking. *Sci. Rep.* **2014**, *4*, 1–11, doi:10.1038/srep07532.
26. Kamińska, A. Molecular characteristics of platelet and urinary extracellular vesicles and their possible applications in nanomedicine. PhD Dissertation, Department of Medical Physics , Faculty of Physics , Astronomy and Applied Computer Science of the Jagiellonian University, Krakow, Poland, **2019**.
27. Pirkmajer, S.; Chibalin, A. V Serum starvation : caveat emptor. **2020**, 272–279, doi:10.1152/ajpcell.00091.2011.
28. Shelke, G.V.; Gho, Y.S. Importance of exosome depletion protocols to eliminate functional and RNA-containing extracellular vesicles from fetal bovine serum. **2014**, *3078*, doi:10.3402/jev.v3.24783.
29. Surman, Kędracka-Krok, S.; Hoja-Łukowicz, D.; Jankowska, U.; Drożdż, A.; Stępień, E.Ł.; Przybyło, M. Mass Spectrometry-Based Proteomic Characterization of Cutaneous Melanoma Ectosomes Reveals the Presence of Cancer-Related Molecules. *Int. J. Mol. Sci.* **2020**, *21*, 2934, doi:10.3390/ijms21082934.
30. Freudenblum, J.; Iglesias, J.A.; Hermann, M.; Walsen, T.; Wilfinger, A.; Meyer, D.; Kimme, R.A. In vivo imaging of emerging endocrine cells reveals a requirement for PI3K-regulated motility in pancreatic islet morphogenesis. *Dev.* **2018**, *145*, doi:10.1242/dev.158477.
31. Freudenblum, J.; Iglesias, J.A.; Hermann, M.; Walsen, T.; Wilfinger, A.; Meyer, D.; Kimme, R.A. In vivo imaging of emerging endocrine cells reveals a requirement for PI3K-regulated motility in pancreatic islet morphogenesis. *Dev.* **2018**, *145*, doi:10.1242/dev.158477.
32. Mihály, J.; Deák, R.; Szigyártó, I.C.; Bóta, A.; Beke-Somfai, T.; Varga, Z. Characterization of extracellular vesicles by IR spectroscopy: Fast and simple classification based on amide and C[sbnd]H stretching vibrations. *Biochim. Biophys. Acta - Biomembr.* **2017**, *1859*, 459–466, doi:10.1016/j.bbamem.2016.12.005.
33. Laurens, L.M.L.; Wolfrum, E.J. Feasibility of spectroscopic characterization of algal lipids: Chemometric correlation of NIR and FTIR Spectra with exogenous lipids in algal biomass. *Bioenergy Res.* **2011**, *4*, 22–35, doi:10.1007/s12155-010-9098-y.
34. Severcan, F.; Harris, P.I. Vibrational Spectroscopy in Diagnosis and Screening. 1st ed. IOS Press, Amsterdam, Netherlands**, 2012**, ISSN 1875-0656.
35. Chiriboga, L.; Xie, P.; Yee, H.; Vigorita, V.; Zarou, D.; Zakim, D.; Diem, M. Infrared spectroscopy of human tissue. I. Differentiation and maturation of epithelial cells in the human cervix. *Biospectroscopy* **1998**, *4*, 47–53, doi:10.1002/(sici)1520-6343(1998)4:1<47::aid-bspy5>3.3.co;2-1.
36. Wang, B.; Xing, D.; Zhu, Y.; Dong, S.; Zhao, B. The State of Exosomes Research: A Global Visualized Analysis. *Biomed Res. Int.* **2019**, *2019*, doi:10.1155/2019/1495130.
37. Ratajczak, J.; Miekus, K.; Kucia, M.; Zhang, J.; Reca, R.; Dvorak, P.; Ratajczak, M.Z. Embryonic stem cell-derived microvesicles reprogram hematopoietic progenitors: Evidence for horizontal transfer of mRNA and protein delivery. *Leukemia* **2006**, *20*, 847–856, doi:10.1038/sj.leu.2404132.
38. Koizume, S.; Ito, S.; Yoshioka, Y.; Kanayama, T.; Nakamura, Y.; Yoshihara, M.; Yamada, R.; Ochiya, T.; Ruf, W.; Miyagi, E.; et al. High-level secretion of tissue factor-rich extracellular vesicles from ovarian cancer cells mediated by filamin-A and protease-activated receptors. *Thromb. Haemost.* **2016**, *115*, 299–310, doi:10.1160/TH15-03-0213.
39. Buschow, S.I.; Nolte-'t Hoen, E.N.M.; van Niel, G.; Pols, M.S.; ten Broeke, T.; Lauwen, M.; Ossendorp, F.; Melief, C.J.M.; Raposo, G.; Wubbolts, R.; et al. MHC II In dendritic cells is targeted to lysosomes or t cell-induced exosomes via distinct multivesicular body pathways. *Traffic* **2009**, *10*, 1528–1542, doi:10.1111/j.1600-0854.2009.00963.x.

40. Buschow, S.I.; Nolte-'t Hoen, E.N.M.; van Niel, G.; Pols, M.S.; ten Broeke, T.; Lauwen, M.; Ossendorp, F.; Melief, C.J.M.; Raposo, G.; Wubbolts, R.; et al. MHC II In dendritic cells is targeted to lysosomes or t cell-induced exosomes via distinct multivesicular body pathways. *Traffic* **2009**, *10*, 1528–1542, doi:10.1111/j.1600-0854.2009.00963.x.
41. Abramowicz, A.; Marczak, L.; Wojakowska, A.; Zapotoczny, S.; Whiteside, T.L.; Widlak, P.; Pietrowska, M. Harmonization of exosome isolation from culture supernatants for optimized proteomics analysis. *PLoS One* **2018**, *13*, 1–15, doi:10.1371/journal.pone.0205496.
42. Lobb, R.J.; Becker, M.; Wen, S.W.; Wong, C.S.F.; Wiegmans, A.P.; Leimgruber, A.; Möller, A. Optimized exosome isolation protocol for cell culture supernatant and human plasma. *J. Extracell. Vesicles* **2015**, *4*, 1–11, doi:10.3402/jev.v4.27031.
43. Grant, R.; Ansa-Addo, E.; Stratton, D.; Antwi-Baffour, S.; Jorfi, S.; Kholia, S.; Krige, L.; Lange, S.; Inal, J. A filtration-based protocol to isolate human Plasma Membrane-derived Vesicles and exosomes from blood plasma. *J. Immunol. Methods* **2011**, *371*, 143–151, doi:10.1016/j.jim.2011.06.024.
44. Lucchetti, D.; Fattorossi, A.; Sgambato, A. Extracellular Vesicles in Oncology: Progress and Pitfalls in the Methods of Isolation and Analysis. *Biotechnol. J.* **2019**, *14*, 1–10, doi:10.1002/biot.201700716.
45. Witwer, K.W.; Buzás, E.I.; Bemis, L.T.; Bora, A.; Lässer, C.; Lötvall, J.; Nolte-'t Hoen, E.N.; Piper, M.G.; Sivaraman, S.; Skog, J.; et al. Standardization of sample collection, isolation and analysis methods in extracellular vesicle research. *J. Extracell. Vesicles* **2013**, *2*, 1–25, doi:10.3402/jev.v2i0.20360.
46. Witwer, K.W.; Buzás, E.I.; Bemis, L.T.; Bora, A.; Lässer, C.; Lötvall, J.; Nolte-'t Hoen, E.N.; Piper, M.G.; Sivaraman, S.; Skog, J.; et al. Standardization of sample collection, isolation and analysis methods in extracellular vesicle research. *J. Extracell. Vesicles* **2013**, *2*, 1–25, doi:10.3402/jev.v2i0.20360.